Perceptual Colors and Textures for Scientific Visualization

Christopher G. Healey
University of California, Berkeley

This talk describes our investigation of methods for choosing color, texture, orientation, shape, and other features to visualize certain types of large, multidimensional datasets. These datasets are becoming more and more common; examples include scientific simulation results, geographic information systems, satellite images, and biomedical scans. The overwhelming amount of information contained in these datasets makes them difficult to analyze using traditional mathematical or statistical techniques. It also makes them difficult to visualize in an efficient or useful manner.

The size of a dataset can be divided into three separate characteristics: the number of elements in the dataset, the number of attributes or dimensions embedded in each element, and the range of values possible for each attribute. All three characteristics may need to be considered during visualization.

Many of our techniques make explicit use of the way viewers perceive information in an image. Our visualization systems display data in a manner that takes advantage of the low-level human visual system. Offloading the majority of the analysis task on the low-level visual system allows users to perform exploratory visualization very rapidly and accurately on large multidimensional datasets. Trends and relationships, unexpected patterns or results, and other areas of interest can be quickly identified within the dataset. These data subsets can then be further visualized or analyzed as required.

Preattentive Processing

One explicit goal of visualization is to present data to human observers in a way that is informative and meaningful, on the one hand, yet intuitive and effortless on the other. Multidimensional data visualization is concerned with the question "How can we display high-dimensional data elements in a low-dimensional environment, such as on a computer screen or the printed page?" This goal is often pursued by attaching "features" such as hue, intensity, spatial location, and size to each data element. Features are chosen to reveal properties of data elements as well as relationships among them. An ad hoc assignment of features to individual data dimensions may not result in a useful visualization tool. Indeed, too often the tool itself interferes with the viewer's ability to extract the desired information due to a poor choice of feature assignment.

One very interesting result of vision research over the past 20 years has been the discovery of a limited set of visual properties that are processed preattentively (*i.e.,* without the need for focused attention). Typically, tasks that can be performed on large multi-element displays in 200 milliseconds or less are considered preattentive. This is because eye movements take at least 200 milliseconds to initiate. Any perception that is possible within this time frame involves only the information available in a single glimpse. Random placement of the elements in the displays ensures that attention cannot be prefocused on any particular location. Observers report that preattentive tasks can be completed with very little effort. Table 1 lists a number of preattentive features, and provides references that describe the tasks that can be performed using these features.

For the purpose of visualization, preattentive features and tasks offer a number of attractive and important benefits:

- preattentive tasks are *rapid* and *accurate*; usually, preattentive tasks can be performed in 200 milliseconds or less with perfect or near-perfect accuracy,

Feature	*Author*
line (blob) orientation	Julész & Bergen (1983); Wolfe (1992)
length	Triesman & Gormican (1988)
width	Julész (1984)
size	Triesman & Gelade (1980)
curvature	Triesman & Gormican (1988)
number	Julész (1985); Trick & Pylyshyn (1994)
terminators	Julész & Bergen (1983)
intersection	Julész & Bergen (1983)
closure	Enns (1986); Triesman & Souther (1986)
color (hue)	Triesman & Gormican (1988); Nagy & Sanchez (1990); D'Zmura (1991)
intensity	Beck et al. (1983); Triesman & Gormican (1988)
flicker	Julész (1971)
direction of motion	Nakayama & Silverman (1986); Driver & McLeod (1992)
binocular lustre	Wolfe & Franzel (1988)
stereoscopic depth	Nakayama & Silverman (1986)
3-D depth cues	Enns (1990)
lighting direction	Enns (1990)

Table 1: A list of two-dimensional features that "pop out" during visual search, and a list of authors who describe preattentive tasks performed using the given feature.

- the time required to perform a preattentive task is *independent of display size*; the number of elements in a display can be increased (to the fidelity of the display device) with little or no increase in the amount of time required to complete the task, and
- experiments in preattentive processing can uncover exactly how different visual features interact with one another; feature preferences, masking effects, and the amount of feature difference required for a specific task can be identified and used to build high-speed visualization tools.

A simple example of a preattentive task is the detection of a filled circle in a group of empty circles (Figure 1a). The target object has the visual feature "filled" but the empty distractor objects do not (all non-target objects are considered distractors). A viewer can tell at a glance whether the target is present or absent.

A conjunction target item is one that is made up of two or more features, only one of which is contained in each of the distractors [43]. Figure 1b shows an example of conjunction search. The target is made up of two features, filled and circular. One of these features is present in each of the distractor objects (filled squares and empty circles). Numerous studies show that the target cannot be preattentively detected, forcing subjects to search serially through the display to find it.

Properties that are processed preattentively can be used to highlight important image characteristics. Experiments in both the cognitive psychology and scientific visualization domains have used various features to assist in performing the following visual tasks:

- *target detection*, where users attempt to rapidly and accurately detect the presence or absence of a "target" element that uses a unique visual feature within a field of distractor elements (Figure 1),

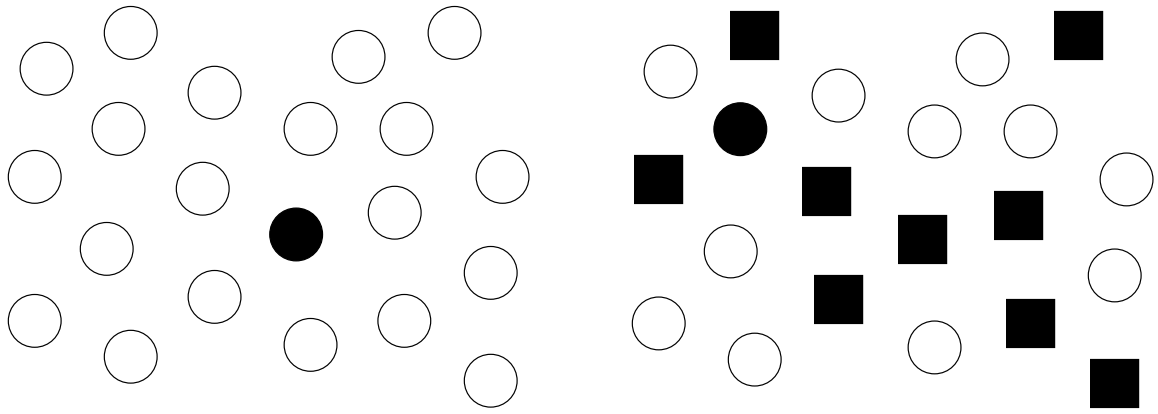

(a) (b)

Figure 1: Examples of two target detection tasks: (a) target can be detected preattentively because it has a unique feature "filled"; (b) target cannot be detected preattentively because it has no visual feature unique from its distractors

- *boundary detection*, where users attempt to rapidly and accurately detect a texture boundary between two groups of elements, where all the elements in each group have a common visual feature (Figure 2), and
- *counting and estimation*, where users attempt to count or estimate the number or percentage of elements in a display that have a unique visual feature.

The conjunction search in Figure 1b shows an example of visual interference, that is, a particular data-feature mapping that hides the information we are interested in studying. Obviously, we want to control or avoid visual interference during visualization. Another example of this problem, feature hierarchy, is shown in Figure 2. In the first display, hue is used to divide the elements into two groups (*i.e.* a red group and a blue group). Form varies randomly from element to element. Tests show it is easy for subjects to identify the hue boundary as either vertical or horizontal. In the second display, the data-feature mapping has been reversed. Form is used to group the elements, and hue varies randomly across the array. It is much harder for subjects to identify the form boundary in these displays. Moreover, it would be difficult to guess beforehand which data-feature mapping would have provided the best performance. Previous studies in preattentive processing could have been used to predict the outcome.

Callaghan [6, 7] first reported the interference effects shown in Figure 2. The visual system seems to prioritize features in order of importance. This means that the presence of visually "important" features can interfere with tasks that use lower priority features. In Figure 2a, the vertical boundary defined by hue is detected preattentively, even though the shape of each element is random. In Figure 2b, however, it is difficult to detect the horizontal boundary defined by form due to random hue variations. If hue were fixed to a constant value for each element, the form boundary could be detected preattentively. Callaghan explains this phenomena by suggesting that the visual system assigns a higher importance to hue than to form during boundary detection. Thus, a random hue interferes with form boundary detection, but a random form has no effect on hue boundary detection. A similar asymmetry exists between hue and intensity. Random hue has no effect on detecting boundaries defined by intensity. However, random intensity interferes with hue boundary detection. Callaghan concluded that intensity is more important than hue to the low-level visual system during boundary identification [5].

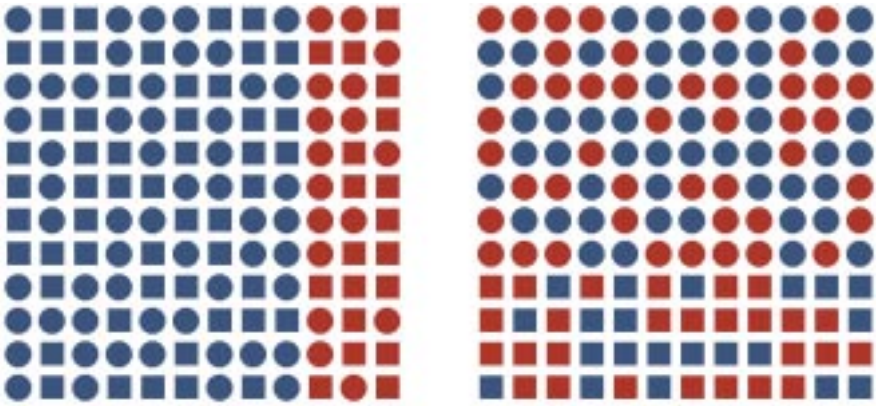

(a) (b)

Figure 2: Region segregation by form and hue: (a) hue boundary is identified preattentively, even though form varies in the two regions; (b) random hue variations interfere with the identification of a region boundary based on form

Researchers continue to expand preattentive processing in a number of exciting directions. To date, most of the features used in preattentive tasks have been relatively simply properties (*e.g.,* hue, orientation, line length, and size). Enns and Rensink, however, have identified a class of three-dimensional elements that can be detected preattentively [10, 11]. They have shown that three-dimensional orientation, shape, and direction of lighting can be used to make elements "pop-out" of a visual scene (Figures 3b and 3c). This is important, because it suggests that complex high-level concepts may be processed preattentively by the low-level visual system.

New tasks that can be performed preattentively are also being investigated. Research has recently been conducted on counting and estimation in preattentive processing. Varey describes experiments in which subjects were asked to estimate the relative frequency of white or black dots [49]. Her results showed that subjects could estimate in four different ways: "percentage" of white dots, "percentage" of black dots, "ratio" of black dots to white dots, and "difference" between the number of black and white dots. She also found that subjects consistently overestimated small proportions and underestimated large proportions. Estimation of relative frequency using hue and orientation was shown to be preattentive in experiments conducted in our laboratory [16, 18]. Moreover, our results showed that there was no feature interaction. Random orientation did not interfere with estimation of targets with a unique hue, and random hue did not interfere with estimation of targets with a unique orientation. This is important because it suggests that hue and orientation can be used to encode two independent data values in a single display without causing visual interference.

A number of scientists have proposed competing theories to explain how preattentive processing occurs, in particular Triesman's feature integration theory [43], Julész' texton theory [23], Quinlan and Humphreys' similarity theory [31], and Wolfe's guided search theory [55]. Our interest is in the use of visual features that have already been shown to be preattentive. Results from psychology are extended, modified, tested, and then integrated into our visualization environment.

Real-Time Preattentive Visualization

Most preattentive techniques are validated by studying a single data frame in isolation. This leads to an interesting question with important relevance to visualization. If a preattentive task can be performed on a single frame in 100

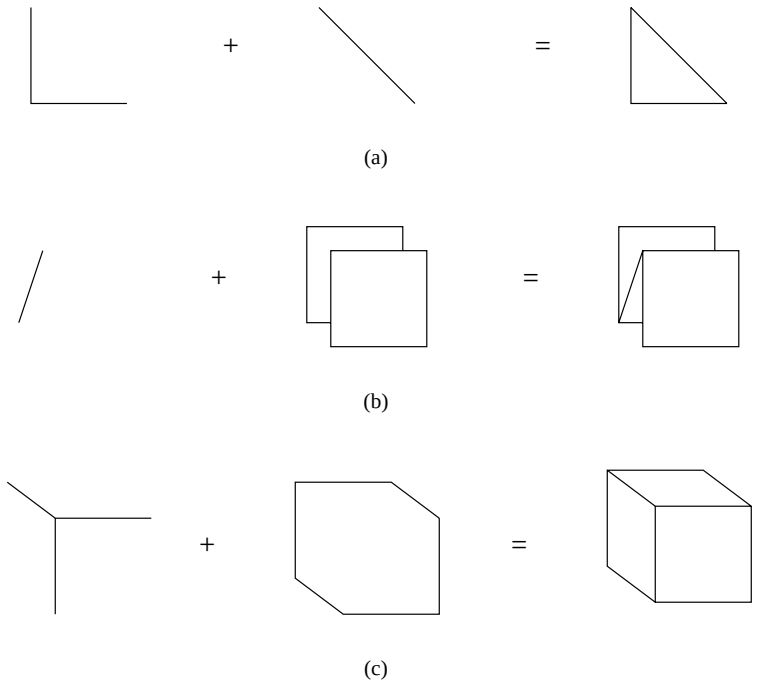

Figure 3: Combination of simple components to form emergent features: (a) closure, a simple closed figure is seen; (b) three-dimensionality, the figure appears to have depth; (c) volume, a solid figure is seen

milliseconds, can the same task can be performed on a real-time sequence of frames displayed at ten frames per second? We hypothesized that important aspects of preattentive processing will extend to a real-time environment. A visualization tool that uses preattentive features will allow viewers to perform visual tasks such as grouping of similar data elements (boundary detection), detection of elements with a unique characteristic (target detection), and estimation of the number of elements with a given value or range of values, all in real-time on temporally animated data frames. We tested this hypothesis using experiments that simulated the use of our preattentive visualization tools in a real-time environment. Analysis of the experimental results supported our hypothesis for boundary and target detection using hue and shape. Moreover, interference properties previously reported for static frames were found to apply to a dynamic environment.

Our initial experiment addressed two general questions about the preattentive features hue and shape, and their use in our visualization tools:

- *Question 1:* Is it possible for subjects to detect a data frame with a horizontal boundary within a sequence of random frames? If so, what features allow this and under what conditions?
- *Question 2:* Do Callaghan's feature hierarchy effects apply to our real-time visualization environment? Specifically, does random hue interfere with form boundary detection within a sequence of frames? Does random form interfere with hue boundary detection within a sequence of frames?

Experimental results showed accurate boundary detection can be performed using either hue or form on sequences of

frames displayed at ten frames per second. Moreover, feature hierarchy effects extended to a dynamic environment, specifically, hue dominated form during boundary detection. A random hue pattern masked form boundaries, while a random form pattern had no effect on hue boundary detection.

A corresponding set of experiments were run to test target detection, with similar results. While both hue and form targets can be detected preattentively in a real-time environment (at frame rates of ten to twenty frames per second), form targets were only visible when the background hue was held constant. Hue variation masked form targets. Form variation had no effect on the detection of hue targets.

We have built a number of visualization tools that allow users to perform exploratory analysis on their datasets in real-time. Experience from using these tools confirmed that our experimental results hold for these datasets and tasks.

Color Selection

Color is a powerful and often-used visual feature. Previous work has addressed the issue of choosing colors for certain types of data visualization. For example, Ware and Beatty describe a simple color visualization technique for displaying correlation in a five-dimensional dataset [51]. Robertson, Ware, Rheingans and Tebbs, and Levkowitz and Herman discuss various methods for building effective color gamuts and colormaps [25, 34, 35, 50]. Recent work at the IBM Thomas J. Watson Research Center has focused on a rule-based visualization tool that considers how a user perceives visual features like hue, luminance, height, and so on [4, 36].

If we use color to represent our data, one important question to ask is: "How can we choose effective colors that provide good differentiation between data elements during the visualization task?" We addressed this problem by trying to answer three related questions:

- How can we allow rapid and accurate identification of individual data elements through the use of color?
- What factors determine whether a "target" element's color will make it easy to find, relative to differently colored "non-target" elements?
- How many colors can we display at once, while still allowing for rapid and accurate target identification?

None of the currently-available color selection techniques were specifically designed to investigate the rapid and accurate identification of individual data elements based on color. Also, since the color gamut and colormap work uses continuous color scales to encode information, they have not addressed the question of how many colors we can effectively display at once, while still providing good differentiation between individual data elements.

We began by using the perceptually balanced CIE LUV color model to provide control over color distance and isoluminance. We also exploited two specific results related to color target detection: linear separation [9, 2] and color category [24]. These effects are controlled to allow for the rapid and accurate identification of color targets. Target identification is a necessary first step towards performing other types of exploratory data analysis. If we can rapidly and accurately differentiate elements based on their color, we can apply our results to other important visualization techniques like detection of data boundaries, the tracking of data regions in real-time, and enumeration tasks like counting and estimation [18, 44, 49].

CIE LUV

The CIE LUV color model was proposed by the Commission Internationale de L'Èclairge (CIE) in 1976 [57]. Colors are specified using the three dimensions L^* (which encodes luminance), u^*, and v^* (which together encode chromaticity). CIE LUV provides two useful properties for controlling perceived color difference. First, colors with the same L^* are isoluminant. Second, Euclidean distance and perceived color difference (specified in ΔE^* units) can be interchanged, since the color difference between two color stimuli x and y (positioned in CIE LUV at (L^*_x, u^*_x, v^*_x) (L^*_y, u^*_y, v^*_y), respectively) is roughly:

$$\Delta E^*_{xy} = \sqrt{(\Delta L^*_{xy})^2 + (\Delta u^*_{xy})^2 + (\Delta v^*_{xy})^2} \tag{1}$$

Linear Separation

The linear separation effect has been described by both D'Zmura and Bauer et. al [2, 9]. D'Zmura was investigating how the human visual system finds a target color in a sea of background non-target colors. D'Zmura ran experiments that asked observers to determine the presence or absence of an orange target. Two groups of differently colored non-target elements were also present in each display (*e.g.*, in one experiment half the non-targets in each display were colored green and half were colored red). Results showed that when the target could be separated by a straight line from its non-targets in color space (Figure 4, target T and non-targets A and C), the time required to determine the target's presence or absence was constant, and independent of the total number of elements being displayed. This suggests detection occurs preattentively in the low-level visual system. When the target was collinear with its non-targets (Figure 4, target T and non-targets A and B), the time required to identify the target was linearly proportional to the number of elements being displayed. Observers had to search serially through each display to determine whether the target was present or absent. Bauer et. al strengthened D'Zmura's results by showing that perceptually balanced color models cannot be used to overcome the linear separation effect. Bauer et. al also replicated their findings in three additional color regions: green, blue, and green-yellow. This suggests linear separation applies to colors from different parts of the visible color domain.

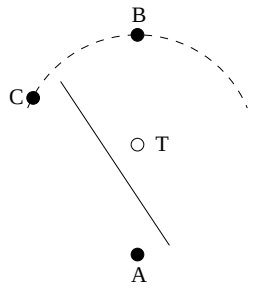

Figure 4: Example of a target with both collinear and separable non-targets, the colors are shown in a u^*, v^*-slice from the CIE LUV color model, notice that target T is equidistant from all three non-targets A, B, and C; in Case 1, target color T is collinear with the non-target colors A and B; in Case 2, target T is linearly separable from its non-targets A and C

Color Category

Kawai et. al [24] reported results that suggest that the time required to identify a color target depends in part on the named color regions occupied by the target and its non-targets. Kawai et. al tested displays that contained a uniquely color target and a constant number of uniformly colored non-targets. They divided an isoluminant, perceptually balanced color slice into named color regions. Their results showed that search times decreased dramatically whenever the non-target was moved outside the target's color region. For example, finding a target colored T in a set of non-targets colored B was significantly more difficult than than finding T in a set of non-targets colored A (Figure 5). Since the target–non-target distances $\overline{TA}$ and $\overline{TB}$ are equal, there was an expectation of perceptual balance that should have been provided by the underlying color model. This expectation was not met. Kawai et. al suggests the difference in performance is due to the fact that both T and B are located in the blue color region, but A is not.

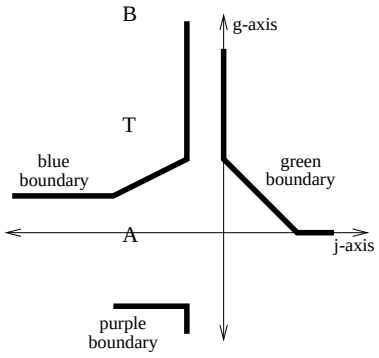

Figure 5: A target T and two non-targets A and B shown in a (j, g) slice from the OSA color model; the boundaries of the blue, green, and purple color regions are shown as thick lines; T and B occupy the same named color region "blue", but A does not

Experiments

We ran a number of experiments to study the effects of color distance, linear separation, and color category. Subjects were shown displays that contained multiple colored squares. Each subject was asked to determine whether a target square with a particular color was present or absent in each display. The experiments were designed to test the following conditions:

- *selection criteria*, which selection criteria (color distance, linear separation, and color category) need to be considered to guarantee equally distinguishable colors,
- *simultaneous colors*, how many colors can we display at the same time, while still allowing users to rapidly and accurately determine the presence or absence of any particular color, and
- *display size*, is performance affected by the number of elements in a display.

We found that up to seven isoluminant colors can be displayed simultaneously, while still allowing for the rapid and accurate identification of any one of the seven. The time required to perform identification was independent of display size, suggesting that target detection is occurring preattentively. Our results also showed that all three selection criteria needed to be considered to guarantee consistent performance. When only some of the selection criteria were used (*e.g.*

only distance and separation, or only category) the amount of time required to identify targets depended on the color of the target: some colors were very easy to identify, while other colors were very difficult. This asymmetry suggested that the colors we chose were not *equally* distinguishable, and therefore that the selection criteria being used were not sufficient to properly control perceived difference between the colors during target detection.

Visualizing CT Medical Scans

One practical application of our color selection technique is the use of color to highlight regions of interest during volume visualization [39]. Radiologists from the University Hospital at the University of British Columbia are studying methods for visualizing abdominal aneurisms. Traditional repair of an abdominal aneurism entails a major operation with an incision into the aneurism, evacuation of the clot contained within, placement of a synthetic graft, and wrapping of the graft with the remnants of the wall of the aneurism. Recently, a new treatment option, endovascular stenting, has been proposed and is currently undergoing clinical trials. This procedure does not require general anesthesia and can be done less invasively by simply placing a self-expanding stent graft via a catheter into the aneurism to stabilize it. Less fit patients are able to withstand the procedure, hospital stay is cut to 1 to 2 days, and post-operative recovery is shortened considerably.

After the operation computed tomography (CT) scans are used to obtain two-dimensional slices of a patient's abdominal region. These slices are reconstructed to produce a three-dimensional volume. The volume is visualized by the radiologists to perform post-operative analysis. A two-pass segmentation step is used to strip out material in each CT slice that does not correspond to one of the regions of interest: the artery running through the abdomen, the aneurism, and the metal hooks (called tynes) used to embed the stent graft within the aneurism. The reconstructed volumes must show clearly each of these three regions.

Normally, greyscale is used to display reconstructed medical volumes. Changes in luminance are most effective for representing the high spatial frequency data contained in these kinds of datasets. For our application, however, one of the most important tasks is identifying the exact position of the tynes (which in turn identify the positions of each of the corresponding stent grafts). In our greyscale volume the location of tynes within the aneurism are obscured by the wall of the aneurism itself (Figure 6a). Different levels of transparency were used to try to "see through" the aneurism, however, we could not find any appropriate value that showed the tyne locations within the artery, while at the same time providing an effective representation of the three-dimensional shape and extent of the wall of the aneurism. We decided that, for this application, it might be more appropriate to high the three regions of interest using color.

Although the radiologists had already chosen a set of colors based on context and aesthetic considerations, it did a poor job of showing the size and shape of the aneurism (Figure 6b). We replaced their colors with three new ones using our color selection technique. The radiologists asked us to avoid greens and green-yellows, since these are associated with bile. We decided to use yellow to represent the artery, purple to represent the aneurism, and red to represent the tynes (Figure 6c). These colors show clearly the location of all three regions of interest within the volume. For example, consider the large patches of yellow within the aneurism. These are areas of "low support"where the grafts in the lower part of the artery were not inserted far enough to mesh with their upstream partner. Although not dangerous, these are exactly the kinds of features the radiologists want to identify during post-operative visualization.

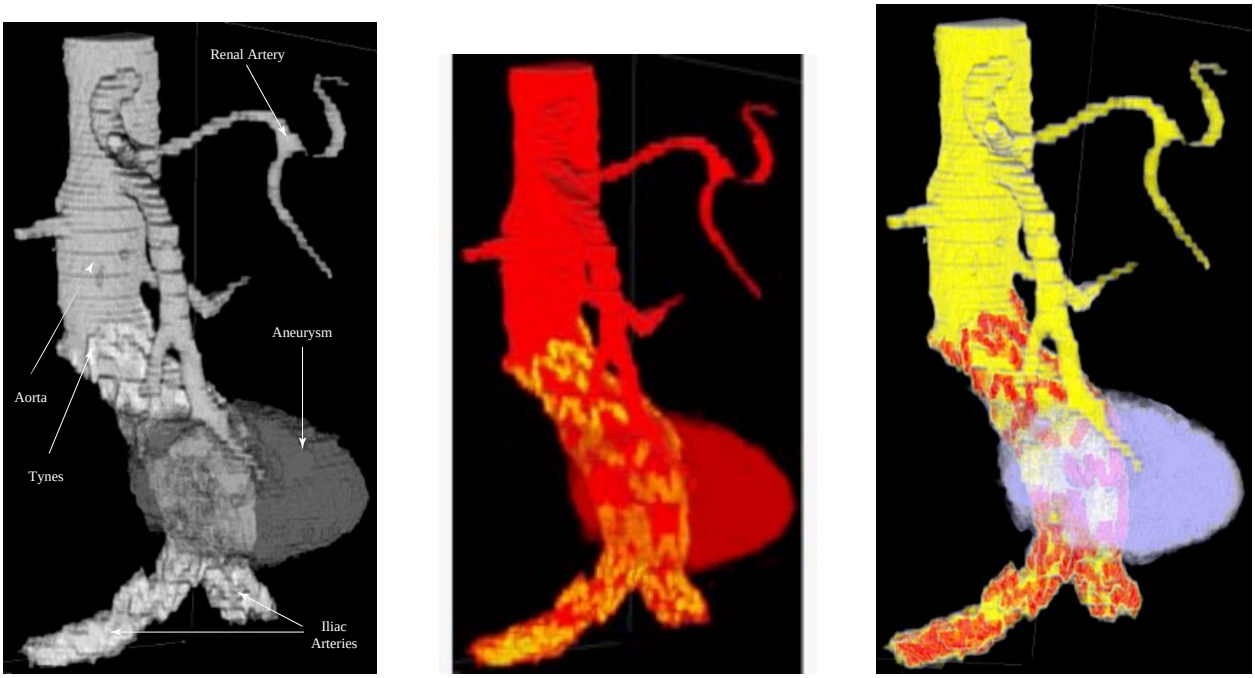

(a) (b) (c)

Figure 6: A reconstructed CT volume showing an abdominal aneurism: (a) greyscale hides the location of the tynes within the aneurism; (b) a color scale chosen by the radiologists obscures the shape and extent of the wall of the aneurism; (c) three colors chosen with our perceptual color selection technique

Perceptual Textures

One of the important issues in scientific visualization is designing methods for representing multiple values (or attributes) at a single spatial location. Although it is possible to assign different visual features to each attribute, simply "stacking" multiple features together will most likely lead to displays that are unintelligible.

Rather than choosing multiple individual features (*i.e.,* color, shape, size, orientation, line length), we decided to try using a single visual feature that could be decomposed into a set of fundamental parts or dimensions. We chose to investigate texture for this purpose.

Texture has been studied extensively in the computer vision, computer graphics, and cognitive psychology communities. Although each group focuses on separate tasks (texture identification and texture segmentation in computer vision, displaying information with texture patterns in computer graphics, and modeling the low-level human visual system in cognitive psychology) they each need ways to describe precisely the textures being identified, classified, or displayed.

Researchers have used different methods to study the perceptual features inherent in a texture pattern. Bela Julész [21] conducted numerous experiments that investigated how a texture's first, second, and third-order statistics affect discrimination in the low-level human visual system. This led to the texton theory [22], which suggests that early vision detects three types of features (or textons, as Julész called them): elongated blobs with specific visual properties (*e.g.,*

hue, orientation, and width), ends of line segments, and crossings of line segments. Tamura et al. [40] and Rao and Lohse [32, 33] identified texture dimensions by conducting experiments that asked subjects to divide pictures depicting different types of textures (Brodatz images) into groups. Tamura et al. used their results to propose methods for measuring coarseness, contrast, directionality, line-likeness, regularity, and roughness. Rao and Lohse used multidimensional scaling to identify the primary texture dimensions used by their subjects to group images: regularity, directionality, and complexity. Haralick et al. [13] built greyscale spatial dependency matrices to identify features like homogeneity, contrast, and linear dependency. These features were used to classify satellite images into categories like forest, woodlands, grasslands, and water. Liu and Picard [26] used Wold features to synthesize texture patterns. A Wold decomposition divides a 2D homogeneous pattern (*e.g.,* a texture pattern) into three mutually orthogonal components with perceptual properties that roughly correspond to periodicity, directionality, and randomness. Malik and Perona [27] designed computer algorithms that use orientation filtering, nonlinear inhibition, and computation of the resulting texture gradient to mimic the discrimination ability of the low-level human visual system. We used these results to choose the perceptual texture dimensions we wanted to investigate during our experiments.

Work in computer graphics has studied methods for using texture patterns to display information during visualization. Schweitzer [38] used rotated discs to highlight the orientation of a three-dimensional surface. Pickett and Grinstein [12] built "stick-men" icons to produce texture patterns that show spatial coherence in a multidimensional dataset. Ware and Knight [52, 53] used Gabor filters to construct texture patterns; attributes in an underlying dataset are used to modify the orientation, size, and contrast of the Gabor elements during visualization. Turk and Banks [48] described an iterated method for placing streamlines to visualize two-dimensional vector fields. Interrante [19] displayed texture strokes to help show three-dimensional shape and depth on layered transparent surfaces; principal directions and curvatures are used to orient and advect the strokes across the surface. Finally, Salisbury et al. [37] and Wikenbach and Salesin [54] used texturing techniques to build computer-generated pen-and-ink drawings that convey a realistic sense of shape, depth, and orientation. We built upon these results to try to develop an effective method for displaying multidimensional data through the use of texture.

Pexels

We wanted to design a technique that will allow users to visualize multidimensional datasets with perceptual textures. To this end, we used a method similar to Ware and Knight to build our displays. Each data element is represented with a single perceptual texture element, or pexel. Our visualization environment consists of a large number of elements arrayed across a three-dimensional surface (*e.g.,* a topographical map or the surface of a three-dimensional object). Each element contains one or more attributes to be displayed. Attribute values are used to control the visual appearance of a pexel by modifying its texture dimensions. Texture patterns formed by groups of spatially neighboring pexels can be used to visually analyze the dataset.

We chose to study three perceptual dimensions: density, regularity, and height. Density and regularity have been identified in the literature as primary texture dimensions [32, 33, 40]. Although height might not be considered an "intrinsic textural cue", we note that height is one aspect of element size, and that element size is an important property of a texture pattern. Moreover, results from cognitive vision have shown that differences in height are detected preattentively by the low-level visual system [1, 43]. We wanted to build three-dimensional pexels that "sit up" on the underlying surface. This allows the possibility of applying various orientations (another important perceptual dimension) to a pexel. Because of this, we chose height as our third texture dimension.

In order to support variation of height, density, and regularity, we built pexels that look like a collection of paper strips. The user maps attributes in the dataset to the density (which controls the number of strips in a pexel), height, and regularity of each pexel. Examples of each of these perceptual dimensions are shown in Figure 7a. Figure 7b shows an

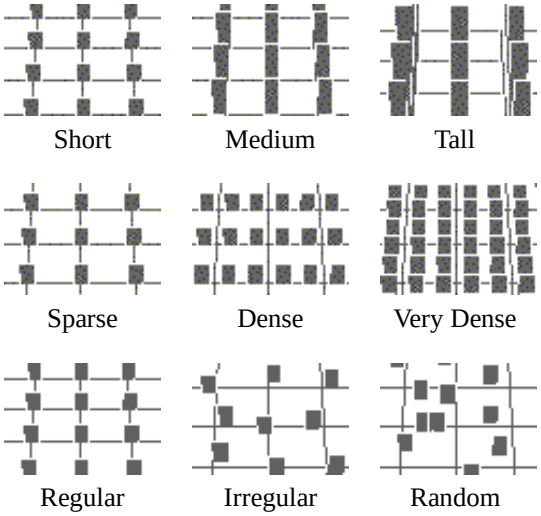

(a)

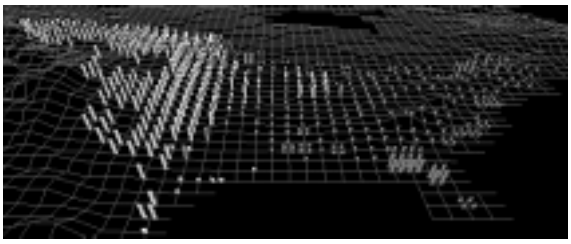

(b)

Figure 7: Groups of paper strips are used to form a pexel that supports variation of the three perceptual texture dimensions height, density and randomness: (a) each pexel has one of its dimensions varied across three discrete values; (b) a map of North America, pexels represent areas of high cultivation, height mapped to level of cultivation, density mapped to ground type, greyscale mapped to vegetation type

environmental dataset visualized with texture and greyscale (we used greyscale for printing purposes only; colour is used to display on-screen images). Locations on the map that contain pexels represent areas in North America with high levels of cultivation. Height shows the level of cultivation (75-99% for short pexels, 100% for tall pexels), density shows the ground type (sparse for alluvial, dense for wetlands), and greyscale shows the vegetation type (dark grey for plains, light grey for forest, and white for woods). Users can easily identify lower levels of cultivation in the central and eastern plains. Areas containing wetlands can be seen as dense pexels in Florida, along the eastern coast, and in the southern parts of the Canadian prairies.

Experiments

In order to test our perceptual dimensions and the interactions that occur between them during visualization, we ran a set of psychophysical experiments. Our experiments were designed to investigate a user's ability to rapidly and accurately identify target pexels defined by a particular height, density, or regularity. Users were asked to determine whether a small group of pexels with a particular type of texture (*e.g.*, a group of taller pexels, as in Figure 8a) was present or absent in a 20×15 array. Conditions like target pexel type, exposure duration, target group size, and background texture dimensions differed for each display. This allowed us to test for preattentive task performance, visual interference, and a user preference for a particular target type. In all cases, user accuracy was used to measure performance.

Design

Each experimental display contained a regularly-spaced 20×15 array of pexels rotated $45°$ about the X-axis (Figure 8). All displays were monochromatic (*i.e.*, grey and white), to avoid variations in color or intensity that might mask the

(a) (b)

Figure 8: Two display types from the taller and regular pexel experiments: (a) a target of medium pexels in a sea of short pexels with a background density pattern (2×2 target group located left of center); (b) a target of regular pexels in a sea of irregular pexels with no background texture pattern (2×2 target group located 8 grids step right and 2 grid steps up from the lower-left corner of the array)

underlying texture pattern. Grid lines were drawn at each row and column, to ensure users perceived the pexels as lying on a tilted 3D plane. After a display was shown, users were asked whether a group of pexels with a particular target value was present or absent. In order to avoid confusion, each user searched for only one type of target pexel: taller, shorter, sparser, denser, more regular, or more irregular. The appearance of the pexels in each display was varied to test for preattentive performance, visual interference, and feature preference. For example, the following experimental conditions were used to investigate a user's ability to identify taller pexels (similar conditions were used for the shorter, denser, sparse, regular, and irregular experiments):

- two target-background pairings: a target of medium pexels in a sea of short pexels, and a target of tall pexels in a sea of medium pexels; different target-background pairings allowed us to test for a subject preference for a particular target type,
- three display durations: 50 msec, 150 msec, and 450 msec; we varied exposure duration to test for preattentive performance, specifically, does the task become more difficult during shorter exposures,
- three secondary texture dimensions: none (every pexel is sparse and regular), density (half the pexels are randomly chosen to be sparse, half to be dense), and regularity (half the pexels are regular, half are random); we added a "background" texture feature to test for visual interference, that is, does the task become more difficult when a secondary texture dimension appears at random spatial locations in the display, and
- two target group sizes: 2×2 pexels and 4×4 pexels; we used different target group sizes to see how large a group of pexels was needed before the target could be detected by a viewer.

Our results suggest that pexels can be used to represent multidimensional data elements, but only if specific data-feature mappings are chosen. Some dimensions were more salient than others, and interference occurred when certain types of pexels were displayed. Specifically, we found that:

- taller pexels can be identified at preattentive exposure durations (*i.e.*, 150 msec or less) with very high accuracy (approximately 93%); background density and regularity patterns produce no significant interference,
- shorter, denser, and sparser pexels are more difficult to identify than taller pexels, although good results are possible at both 150 and 450 msec; height, regularity, and density background texture patterns cause interference for all three target types,

- irregular pexels are difficult to identify, although reasonable accuracy (approximately 76%) is possible at 150 and 450 msec with no background texture pattern, and
- regular pexels cannot be accurately identified; the percentage of correct results approached chance (*i.e.*, 50%) for every condition.

These results suggest that height and density can be used to to form texture patterns that can be identified preattentively. Regularity, however, can only be used as a secondary dimension. While differences in regularity cannot be detected consistently by the low-level visual system, in many cases users will be able to see changes in regularity when areas of interest in a dataset are identified and analyzed in a focused or attentive fashion.

Visualizing Typhoon Data

One of our current testbeds for using pexels to visualize multidimensional data is the analysis of environmental conditions related to typhoons. We used pexels to visualize typhoon activity in the Northwest Pacific Ocean during the summer and fall of 1997. The names "typhoon" and "hurricane" are region-specific, and refer to the same type of weather phenomena: an atmospheric disturbance characterized by low pressure, thunderstorm activity, and a cyclic wind pattern. Storms of this type with windspeeds below 17m/s are called "tropical depressions". When windspeeds exceed 17m/s, they become "tropical storms". This is also when storms are assigned a specific name. When windspeeds reach 33m/s, a storm becomes a typhoon (in the Northwest Pacific) or a hurricane (in the Northeast Pacific and North Atlantic).

We combined information from a number of different sources to collect the data we needed. A U.S. Navy elevation dataset[1] was used to obtain land elevations at ten minute latitude and longitude intervals. Land-based weather station readings collected from around the world and archived by the National Climatic Data Center[2] provided daily measurements for eighteen separate environmental conditions. Finally, satellite archives made available by the Global Hydrology and Climate Center[3] contained daily open-ocean windspeed measurements at thirty minute latitude and longitude intervals. The National Climatic Data Center defined the 1997 typhoon season to run from August 1 to October 31; each of our datasets contained measurements for this time period.

We chose to visualize three environmental conditions related to typhoons: windspeed, pressure, and precipitation. All three values were measured on a daily basis at each land-based weather station, but only daily windspeeds were available for open-ocean positions. In spite of the missing open-ocean pressure and precipitation, we were able to track storms as they moved across the Northwest Pacific Ocean. When the storms made landfall the associated windspeed, sea-level pressure, and precipitation were provided by weather stations along their path.

Based on our experimental results, we chose to represent windspeed, pressure, and precipitation with height, density, and regularity, respectively. Localized areas of high windspeed are an obvious indicator of storm activity. We chose to map increasing windspeed to an increased pexel height. Our experimental results showed that taller pexels can be identified preattentively, regardless of any background texture pattern that might be present. Windspeed has two important boundaries: 17m/s (where tropical depressions become tropical storms) and 33m/s (where storms become typhoons). We mirrored these boundaries with height discontinuities. Pexel height increases linearly from 0-17m/s. At 17m/s, height approximately doubles, then continues linearly from 17-33m/s. At 33m/s another height discontinuity is introduced, followed by a linear increase for any windspeeds over 33m/s.

[1] http://grid2.cr.usgs.gov/dem/

[2] http://www.ncdc.noaa.gov/ol/climate/online/gsod.html

[3] http://ghrc.msfc.nasa.gov/ims-cgi-bin/execute?mkinfo+mif13owsg

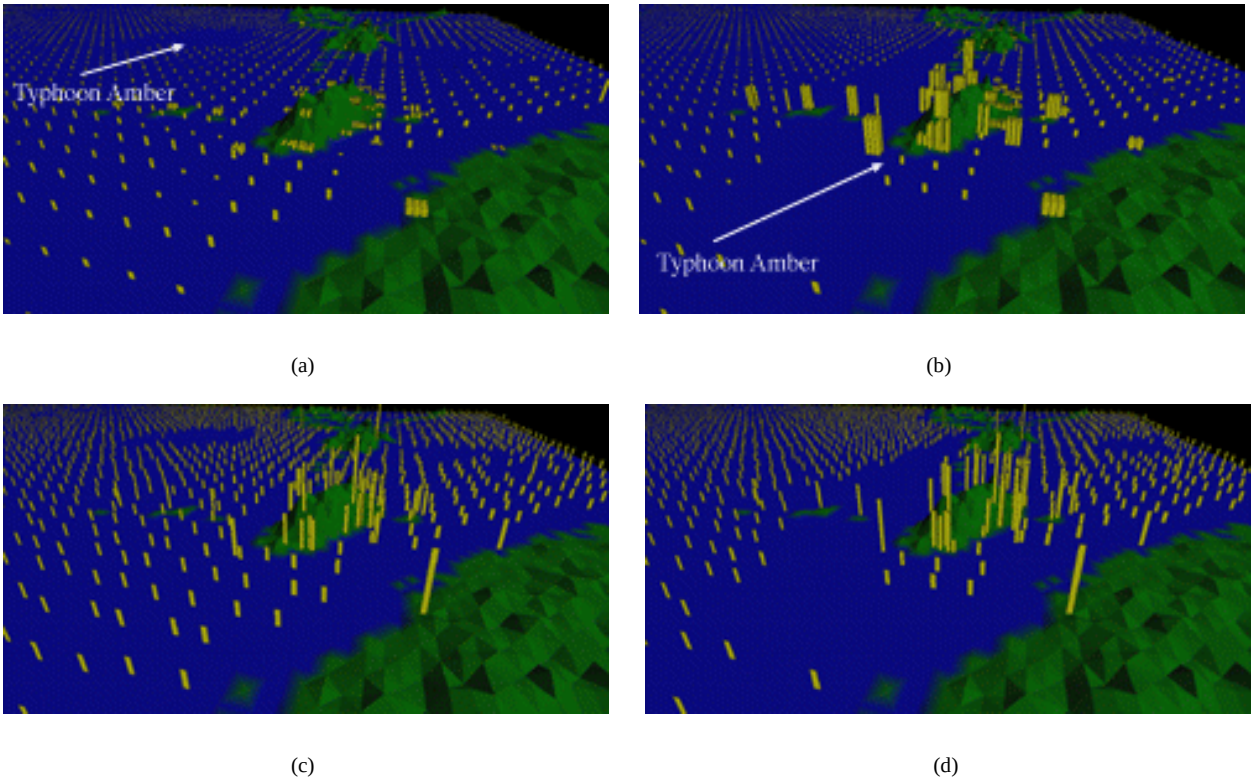

Figure 9: (a) windspeed mapped to height, pressure mapped to density, precipitation mapped to regularity: looking south, typhoon Amber moves east to west across the Northwest Pacific (August 26, 1997); (b) typhoon Amber makes landfall on the island of Taiwan (August 28, 1997); (c, d) same data as for (a) and (b), but with windspeed mapped to regularity, pressure mapped to height, precipitation mapped to density: the use of regularity makes it significantly more difficult to track typhoons when they make landfall

Pressure is represented with pexel density. An increase in pressure is mapped to a decrease in pexel density (*i.e.*, very dense pexels represent areas of very low pressure). Pressure below 996 millibars produces very dense pexels. Pressure between 996 and 1014 millibars is represented by dense pexels. Pressure over 1014 millibars results in sparse pexels. Our experimental results showed it was easier to find dense pexels in a sea of sparse pexels, as opposed to sparse in dense. Our mapping uses high-density pexels to highlight the low-pressure areas associated with typhoon activity.

Precipitation is represented with pexel regularity. High levels of precipitation result in an irregular pexel pattern. Pexel positions are held regular for a daily rainfall of 0.13 inches or less (the median value for the time period we visualized). Daily rainfall over 0.13 inches produces an increased pexel irregularity. Because precipitation was not as important as either windspeed or pressure during visualization, it was assigned to our least effective texture dimension, regularity.

We built a simple visualization tool that maps windspeed, pressure, and precipitation to their corresponding height, density, and regularity. Our visualization tool allows a user to move forwards and backwards through the dataset day-by-day. One interesting result was immediately evident when we began our analysis: typhoon activity was not represented by high windspeed values in our open-ocean dataset. Typhoons normally contain severe rain and thunderstorms. The high levels of cloud-based water vapor produced by these storms block the satellites that are used to measure open-ocean windspeeds. The result is an absence of any windspeed values within a typhoon's spatial extent. Rather than appearing as a local region of high windspeeds, typhoons on the open-ocean are displayed as a "hole", an ocean region

without any windspeed readings (see Figures 9a and 9b). This absence of a visual feature (*i.e.*, a hole in the texture field) is large enough to be salient in our displays, and can be preattentively identified and tracked over time. Therefore, users have little difficulty finding storms and watching them as they move across the open ocean. When a storm makes landfall, the weather stations along the storm's path provide the proper windspeed, as well as pressure and precipitation. Weather stations measure windspeed directly, rather than using satellite images, so high levels of cloud-based water vapor cause no loss of information.

Two display frames from our visualization tool are shown in Figure 9. Figure 9a, looking south, tracks typhoon Amber (one of the region's major typhoons) approaching along an east to west path across the Northwest Pacific Ocean on August 26, 1997. Figure 9b shows typhoon Amber two days later as it moves through Taiwan. Weather stations within the typhoon show the expected strong winds, low pressure, and high levels of rainfall. These results are easily identified as tall, dense, irregular pexels. Compare these images to Figures 9c-d, where windspeed was mapped to regularity, pressure to height, and precipitation to density (a mapping that our experiments predict will perform poorly). Although viewers can identify areas of lower and higher windspeed (*e.g.*, on the open ocean and over Taiwan), it is difficult to identify *a change* in lower or higher windspeeds (*e.g.*, the change in windspeed as typhoon Amber moves onshore over Taiwan). In fact, viewers often searched for an increase in height that represents a decrease in pressure, rather than an increase in irregularity; pexels over Taiwan become noticeably taller between Figures 9c and 9d.

Oceanography Simulations

Our final example describes a set of oceanography simulations being jointly conducted at North Carolina State University and the University of British Columbia [15]. Researchers in oceanography are studying the growth and movement patterns of different species of salmon in the northern Pacific Ocean. Underlying environmental conditions like plankton density, sea surface temperature (SST), current direction, and current strength affect where the salmon live and how they move and grow [41]. For example, salmon like cooler water and tend to avoid ocean locations above a certain temperature. Since the salmon feed on plankton blooms, they will try to move to areas where plankton density is highest. Currents will "push" the salmon as they swim. Finally, SST, current direction, and current strength affect the size and location of plankton blooms as they form.

The oceanographers are designing models of how they believe salmon feed and move in the open ocean. These simulated salmon will be placed in a set of known environmental conditions, then tracked to see if their behavior mirrors that of the real fish. For example, salmon that migrate back to the Fraser River to spawn chose one of two routes. When the Gulf of Alaska is warm, salmon make landfall at the north end of Vancouver Island and approach the Fraser River primarily via a northern route through the Johnstone Strait (the upper arrow in Figure 10). When the Gulf of Alaska is cold, salmon are distributed further south, make landfall on the west coast of Vancouver Island, and approach the Fraser River primarily via a southern route through the Juan de Fuca Strait (the lower arrow in Figure 10). The ability to predict salmon distributions from prevailing environmental conditions would allow the commercial fishing fleet to estimate how many fish will pass through the Johnstone and Juan de Fuca straits. It would also allow more accurate predictions of the size of the salmon run, helping to ensure that an adequate number of salmon arrive at the spawning grounds.

In order to test their hypotheses, the oceanographers have created a database of SSTs and ocean currents for the region 35° north latitude, 180° west longitude to 62° north latitude, 120° west longitude (Figure 10). Measurements within this region are available at $1^\circ \times 1^\circ$ grid spacings. This array of values exists for each month for the years 1956 to 1964, and 1980 to 1989.

Partial plankton densities have also been collected and tabulated; these are obtained by ships that take readings at vari-

Figure 10: Map of the North Pacific; arrows represent possible salmon migration paths as they pass through the either Johnstone Strait (upper arrow) or the Strait of Juan de Fuca (lower arrow)

ous positions in the ocean. We estimated missing plankton values using a set of knowledge discovery (KD) algorithms that we have specifically modified for use during visualization. Our KD algorithms identified month, SST, and current magnitude as the attributes used to estimate missing plankton values. Because of this, we restricted our initial visualization to a monthly time-series of plankton density, SST, and current magnitude.

Displaying the three attributes together allows the oceanographers to search for relationships between plankton density, current strength, and SST. Plankton is displayed using colour; SST and current strength are displayed using texture. Colours for the five plankton ranges were chosen using our colour selection technique [14]. Although other colour scales were available (for example, by Ware [50]), our colours are specifically designed to highlight outliers, and to show clearly the boundaries between groups of elements with a common plankton density. We display the five plankton density ranges from low to high using blue (monitor RGB=36, 103, 151), green (monitor RGB=18, 127, 45), brown (monitor RGB=134, 96, 1), red (monitor RGB=243, 51, 55), and purple (monitor RGB=206, 45, 162),

For the underlying texture, we mapped current strength to height and SST to density. Our choices were guided by results we observed from our texture experiments:

- differences in height (specifically, taller elements) may be easier to detect, compared to differences in density or randomness,
- variation in height may mask differences in density or randomness; this appears to be due to the occlusion that occurs when tall pexels in the foreground hide short pexels in the background; this will be less important when users can control their viewpoint into the dataset (our visualization tool allows the user to interactively manipulate the viewpoint), and
- tightly spaced grids can support up to three easily distinguishable density patterns; placing more strips in a single pexel (*e.g.*, arrays of 3×3 or 4×4 strips) will either cause the strips to overlap with their neighbors, or make each strip too thin to easily identify.

Because there may be a feature preference for height over density, and because current strength was deemed "more important" than SST during knowledge discovery, we used height to represent currents and density to represent SSTs. The five ranges of current strength are mapped to five different heights. We do not use a linear mapping, rather the lower two ranges (corresponding to the weakest currents) are displayed using two types of short pexels, and the upper three ranges (corresponding to the strongest currents) are displayed using three types of tall pexels. This allows a user to rapidly locate boundaries between weak and strong currents, while still being able to identify each of the five ranges. For SSTs, the lower three ranges (corresponding to the coldest SSTs) are displayed with a pexel containing a single strip, while the upper two ranges (corresponding to the warmest SSTs) are displayed with pexels containing arrays of 2×1 and 2×2 strips, respectively. The densities we chose allow a user to see clearly the boundaries between cold and warm temperature regions. If necessary, users can change the range boundaries to focus on different SST gradients.

The oceanographers want to traverse their datasets in monthly and yearly steps. Experiments run in our laboratory have shown that preattentive tasks performed on static frames can be extended to a dynamic environment, where displays are shown one after another in a movie-like fashion [17]. Our visualization tool was designed to allow users to scan rapidly forwards and backwards through the dataset. This makes it easy to compare changes in the value and location of any of the environmental variables being displayed. The oceanographers can track seasonal changes in current strength, SST, and plankton density as they move month by month through a particular year. They can also see how interannual variability affects the environmental conditions and corresponding plankton densities for a particular month across a range of years.

Figure 11 shows three frames from the oceanography dataset: February 1956, June 1956, and October 1956. Colour shows the seasonal variation in plankton densities. Height and density allow the oceanographers to track current strengths and SSTs. In February (Figure 11a), most plankton densities are less than 28 g/m^3 (*i.e.*, blue and green strips). Currents are low in the north-central Pacific; a region of weak currents also sits off the south coast of Alaska. Most of the ocean is cold (sparse pexels), although a region of higher temperatures can easily be seen as dense pexels in the south. In June (Figure 11b) dense plankton blooms (red and purple strips) are present across most of the northern Pacific. The positions of the strong currents have shifted (viewing the entire dataset shows this current pattern is relatively stable for the months March to August). Warmer SSTs have pushed north, although the ocean around Alaska and northern British Columbia is still relatively cold. By October the plankton densities have started to decrease (green, brown, and red strips); few high or low density patches are visible. Current strengths have also decreased in the eastern regions. Overall a much larger percentage of the ocean is warm (*i.e.*, dense pexels). This is common, since summer temperatures will sometimes last in parts of the ocean until October or November.

References

[1] AKS, D. J., AND ENNS, J. T. Visual search for size is influenced by a background texture gradient. *Journal of Experimental Psychology: Perception and Performance 22*, 6 (1996), 1467–1481.

[2] BAUER, B., JOLICOEUR, P., AND COWAN, W. B. Visual search for colour targets that are or are not linearly-separable from distractors. *Vision Research* (1996), (in press).

[3] BECK, J., PRAZDNY, K., AND ROSENFELD, A. A theory of textural segmentation. In *Human and Machine Vision*, J. Beck, K. Prazdny, and A. Rosenfeld, Eds. Academic Press, New York, New York, 1983, pp. 1–39.

[4] BERGMAN, L. D., ROGOWITZ, B. E., AND TREINISH, L. A. A rule-based tool for assisting colormap selection. In *Proceedings Visualization '95* (Atlanta, Georgia, 1995), pp. 118–125.

[5] CALLAGHAN, T. C. Dimensional interaction of hue and brightness in preattentive field segregation. *Perception & Psychophysics 36*, 1 (1984), 25–34.

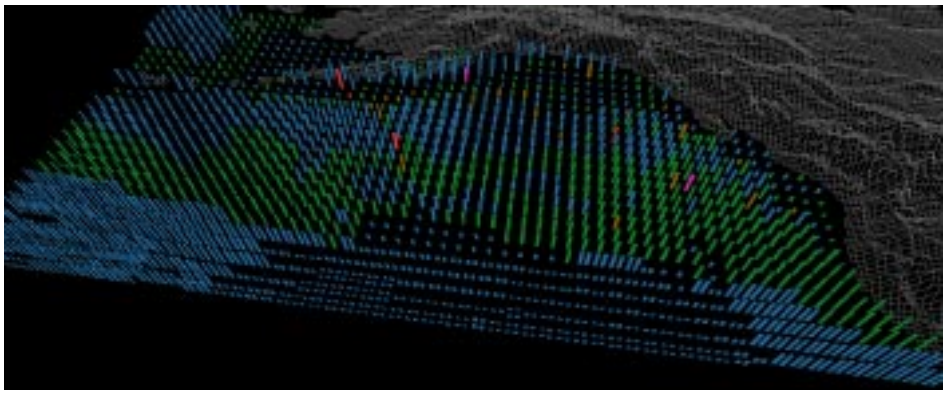

(a)

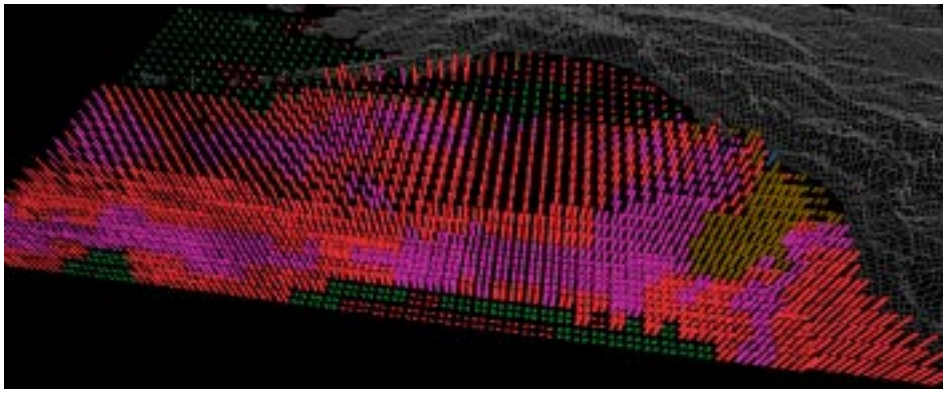

(b)

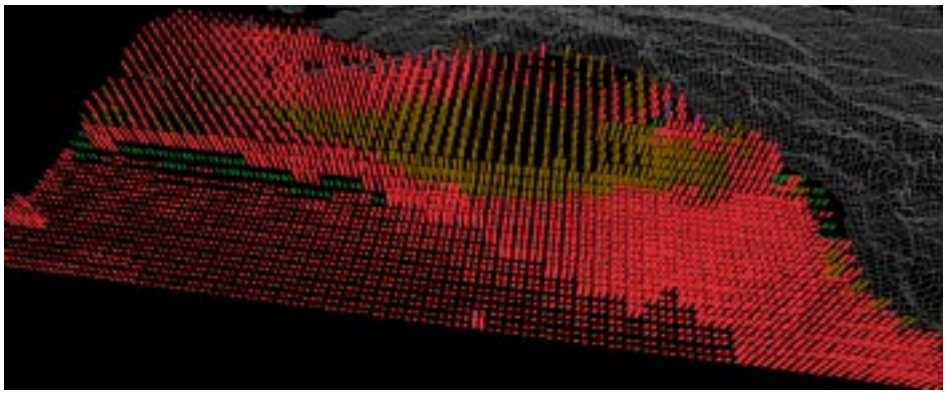

(c)

Figure 11: Visualization of the oceanography datasets, colour used to represent plankton density (blue, green, brown, red, and purple represent lowest to highest densities), height used to represent current strength, texture density used to represent SST: (a) February, 1956; (b) June, 1956; (c) October, 1956

[6] CALLAGHAN, T. C. Interference and domination in texture segregation: Hue, geometric form, and line orientation. *Perception & Psychophysics 46*, 4 (1989), 299–311.

[7] CALLAGHAN, T. C. Interference and dominance in texture segregation. In *Visual Search*, D. Brogan, Ed. Taylor & Francis, New York, New York, 1990, pp. 81–87.

[8] DRIVER, J., MCLEOD, P., AND DIENES, Z. Motion coherence and conjunction search: Implications for guided search theory. *Perception & Psychophysics 51*, 1 (1992), 79–85.

[9] D'ZMURA, M. Color in visual search. *Vision Research 31*, 6 (1991), 951–966.

[10] ENNS, J. T. The promise of finding effective geometric codes. In *Proceedings Visualization '90* (San Francisco, California, 1990), pp. 389–390.

[11] ENNS, J. T., AND RENSINK, R. A. Sensitivity to three-dimensional orientation in visual search. *Psychology Science 1*, 5 (1990), 323–326.

[12] GRINSTEIN, G., PICKETT, R., AND WILLIAMS, M. EXVIS: An exploratory data visualization environment. In *Proceedings Graphics Interface '89* (London, Canada, 1989), pp. 254–261.

[13] HARALICK, R. M., SHANMUGAM, K., AND DINSTEIN, I. Textural features for image classification. *IEEE Transactions on System, Man, and Cybernetics SMC-3*, 6 (1973), 610–621.

[14] HEALEY, C. G. Choosing effective colours for data visualization. In *Proceedings Visualization '96* (San Francisco, California, 1996), pp. 263–270.

[15] HEALEY, C. G. One the use of perceptual cues and data mining for effective visualization of scientific datasets. In *Proceedings Graphics Interface '98* (Vancouver, Canada, 1998), p. (to appear).

[16] HEALEY, C. G., BOOTH, K. S., AND ENNS, J. T. Harnessing preattentive processes for multivariate data visualization. In *Proceedings Graphics Interface '93* (Toronto, Canada, 1993), pp. 107–117.

[17] HEALEY, C. G., BOOTH, K. S., AND ENNS, J. T. Real-time multivariate data visualization using preattentive processing. *ACM Transactions on Modeling and Computer Simulation 5*, 3 (1995), 190–221.

[18] HEALEY, C. G., BOOTH, K. S., AND ENNS, J. T. High-speed visual estimation using preattentive processing. *ACM Transactions on Computer-Human Interaction 3*, 2 (1996), 107–135.

[19] INTERRANTE, V. Illustrating surface shape in volume data via principle directon-driven 3d line integral convolution. In *SIGGRAPH 97 Conference Proceedings* (Los Angeles, California, 1997), T. Whitted, Ed., pp. 109–116.

[20] JULÉSZ, B. *Foundations of Cyclopean Perception*. University of Chicago Press, Chicago, Illinois, 1971.

[21] JULÉSZ, B. A theory of preattentive texture discrimination based on first-order statistics of textons. *Biological Cybernetics 41* (1981), 131–138.

[22] JULÉSZ, B. A brief outline of the texton theory of human vision. *Trends in Neuroscience 7*, 2 (1984), 41–45.

[23] JULÉSZ, B., AND BERGEN, J. R. Textons, the fundamental elements in preattentive vision and perception of textures. *The Bell System Technical Journal 62*, 6 (1983), 1619–1645.

[24] KAWAI, M., UCHIKAWA, K., AND UJIKE, H. Influence of color category on visual search. In *Annual Meeting of the Association for Research in Vision and Ophthalmology* (Fort Lauderdale, Florida, 1995), p. #2991.

[25] LEVKOWITZ, H., AND HERMAN, G. T. Color scales for image data. *IEEE Computer Graphics & Applications 12*, 1 (1992), 72–80.

[26] LIU, F., AND PICARD, R. W. Periodicity, directionality, and randomness: Wold features for perceptual pattern recognition. In *Proceedings 12th International Conference on Pattern Recognition* (Jerusalem, Israel, 1994), pp. 1–5.

[27] MALIK, J., AND PERONA, P. Preattentive texture discrimination with early vision mechanisms. *Journal of the Optical Society of America A 7*, 5 (1990), 923–932.

[28] NAGY, A. L., AND SANCHEZ, R. R. Critical color differences determined with a visual search task. *Journal of the Optical Society of America A 7*, 7 (1990), 1209–1217.

[29] NAGY, A. L., SANCHEZ, R. R., AND HUGHES, T. C. Visual search for color differences with foveal and peripheral vision. *Journal of the Optical Society of America A 7* (1990), 1995–2001.

[30] NAKAYAMA, K., AND SILVERMAN, G. H. Serial and parallel processing of visual feature conjunctions. *Nature 320* (1986), 264–265.

[31] QUINLAN, P. T., AND HUMPHREYS, G. W. Visual search for targets defined by combinations of color, shape, and size: An examination of task constraints on feature and conjunction searches. *Perception & Psychophysics 41*, 5 (1987), 455–472.

[32] RAO, A. R., AND LOHSE, G. L. Identifying high level features of texture perception. *CVGIP: Graphics Models and Image Processing 55*, 3 (1993), 218–233.

[33] RAO, A. R., AND LOHSE, G. L. Towards a texture naming system: Identifying relevant dimensions of texture. In *Proceedings Visualization '93* (San Jose, California, 1993), pp. 220–227.

[34] RHEINGANS, P., AND TEBBS, B. A tool for dynamic explorations of color mappings. *Computer Graphics 24*, 2 (1990), 145–146.

[35] ROBERTSON, P. K. Visualizing color gamuts: A user interface for the effective use of perceptual color spaces in data displays. *IEEE Computer Graphics & Applications 8*, 5 (1988), 50–64.

[36] ROGOWITZ, B. E., AND TREINISH, L. A. An architecture for rule-based visualization. In *Proceedings Visualization '93* (San Jose, California, 1993), pp. 236–243.

[37] SALISBURY, M., WONG, M. T., HUGHES, J. F., AND SALESIN, D. H. Orientable textures for image-based pen-and-ink illustration. In *SIGGRAPH 97 Conference Proceedings* (Los Angeles, California, 1997), T. Whitted, Ed., pp. 401–406.

[38] SCHWEITZER, D. Artifical texturing: An aid to surface visualization. *Computer Graphics (SIGGRAPH 83 Conference Proceedings) 17*, 3 (1983), 23–29.

[39] TAM, R., HEALEY, C. G., AND FLAK, B. Volume visualization of abdominal aortic aneurysms. In *Proceedings Visualization '97* (Phoenix, Arizona, 1997), pp. 43–50.

[40] TAMURA, H., MORI, S., AND YAMAWAKI, T. Textural features corresponding to visual perception. *IEEE Transactions on Systems, Man, and Cybernetics SMC-8*, 6 (1978), 460–473.

[41] THOMSON, K. A., INGRAHAM, W. J., HEALEY, M. C., LEBLOND, P. H., GROOT, C., AND HEALEY, C. G. Computer simulations of the influence of ocean currents on Fraser River sockeye salmon (*oncorhynchus nerka*) return times. *Canadian Journal of Fisheries and Aquatic Sciences 51*, 2 (1994), 441–449.

[42] TRICK, L., AND PYLYSHYN, Z. Why are small and large numbers enumerated differently? A limited capacity preattentive stage in vision. *Psychology Review 101* (1994), 80–102.

[43] TRIESMAN, A. Preattentive processing in vision. *Computer Vision, Graphics and Image Processing 31* (1985), 156–177.

[44] TRIESMAN, A. Search, similarity, and integration of features between and within dimensions. *Journal of Experimental Psychology: Human Perception & Performance 17*, 3 (1991), 652–676.

[45] TRIESMAN, A., AND GELADE, G. A feature-integration theory of attention. *Cognitive Psychology 12* (1980), 97–136.

[46] TRIESMAN, A., AND GORMICAN, S. Feature analysis in early vision: Evidence from search asymmetries. *Psychological Review 95*, 1 (1988), 15–48.

[47] TRIESMAN, A., AND SOUTHER, J. Illusory words: The roles of attention and top-down constraints in conjoining letters to form words. *Journal of Experimental Psychology: Human Perception & Performance 14* (1986), 107–141.

[48] TURK, G., AND BANKS, D. Image-guided streamline placement. In *SIGGRAPH 96 Conference Proceedings* (New Orleans, Louisiana, 1996), H. Rushmeier, Ed., pp. 453–460.

[49] VAREY, C. A., MELLERS, B. A., AND BIRNBAUM, M. H. Judgments of proportions. *Journal of Experimental Psychology: Human Perception & Performance 16*, 3 (1990), 613–625.

[50] WARE, C. Color sequences for univariate maps: Theory, experiments, and principles. *IEEE Computer Graphics & Applications 8*, 5 (1988), 41–49.

[51] WARE, C., AND BEATTY, J. C. Using colour dimensions to display data dimensions. *Human Factors 30*, 2 (1988), 127–142.

[52] WARE, C., AND KNIGHT, W. Orderable dimensions of visual texture for data display: Orientation, size, and contrast. In *Proceedings SIGCHI '92* (Monterey, California, 1992), pp. 203–209.

[53] WARE, C., AND KNIGHT, W. Using visual texture for information display. *ACM Transactions on Graphics 14*, 1 (1995), 3–20.

[54] WINKENBACH, G., AND SALESIN, D. H. Rendering free-form surfaces in pen-and-ink. In *SIGGRAPH 96 Conference Proceedings* (New Orleans, Louisiana, 1996), H. Rushmeier, Ed., pp. 469–476.

[55] WOLFE, J. M. Guided Search 2.0: A revised model of visual search. *Psychonomic Bulletin & Review 1*, 2 (1994), 202–238.

[56] WOLFE, J. M., FRIEDMAN-HILL, S. R., STEWART, M. I., AND O'CONNELL, K. M. The role of categorization in visual search for orientation. *Journal of Experimental Psychology: Human Perception & Performance 18*, 1 (1992), 34–49.

[57] WYSZECKI, G., AND STILES, W. S. *Color Science: Concepts and Methods, Quantitative Data and Formulae, 2nd Edition*. John Wiley & Sons, Inc., New York, New York, 1982.